Modulation of Tris(*o*-phenylenedioxy)cyclotrisphosphazene (TPP) Properties for Zeolite Use: Effect of π-Conjugation Length and CH/N Heterosubstitution

Godefroid Gahungu,[†,‡] Jingping Zhang,*[,†] Bin Zhang,[§] and Theophile Ndikumana[‡]

Faculty of Chemistry, Northeast Normal University, 5268 Renmin Street, Changchun 130024, China, Département de Chimie, Université du Burundi, BP 2700 Bujumbura, Burundi, and Organic Solid Laboratory, CMS Institute of Chemistry, Beijing 100080, China

Received: May 12, 2008; Revised Manuscript Received: October 10, 2008

Highly accurate quantum chemical calculations were used in a comparative study of the π-conjugation length and CH/N heterosubstitution effects on the structure and a number of properties of tris(*o*-phenylenedioxy) cyclotrisphosphazene (TPP) derivatives to identify the role of each of them in the modulation of the host···guest complex stability and available space for the adsorbate within TPP-like organic zeolite (OZ). From the BH&HLYP/6-31G(d,p) structures it was found that extending the side fragment with a phenyl ring and substituting CH/N preserve the "paddle wheel" molecular shape, a key factor in the tunnel formation on which the organic zeolite use of TPP is based on. Compared to the unsubstituted molecules, the side fragment is shortened for CH/N heterosubstitution, which may decrease the diameter of the tunnel. In addition, through accurate ionization potential (IP) calculations (at the HF/6-311+G(d) level) the electron-donor (E-D) capacity was found to be more significantly enhanced by a lateral than a linear extension with phenyl ring, while it decreased upon CH/N heterosubstitution, which can affect the stability of some related host···guest complexes in the same order. Finally, as recently reported for TPP, the current results based on PBE0/6-31G(d,p) show that upon release of an electron the structural stability may not be altered by a CH/N mono- or disubstitution. From these features it was concluded that if the crystal requirement can be attained clathrates of good tolerance toward guest molecules in a wide range of Lewis acidity with variable E-D strength and available space for adsorbates may be reasonably awaited by exploiting these two approaches.

1. Introduction

Formed by three or more −P═N− units, cyclophosphazenes are cyclic compounds[1,2] that have been revealed to be very versatile materials.[3−5] Such diverse structures as clathrates,[6] ionic conductors,[7] ion receptors,[8] or dendrimers[9,10] have been prepared using cyclophosphazene units, and researchers have realized that these can be used as building blocks for preparation of self-assembled materials.[11] As a result of their unique features, organic zeolites (OZ) and molecular self-assembled materials[12,13] seem to constitute a competing alternative for strategic industrial and environmental applications such as gas storage, selective gas recognition, and separation, where absorption properties of materials are emerging as a forefront issue of present-day research.[14−16] Thus far it has been reported that these can be prepared simply by exploiting soft interactions: the ease of formation results in a surprising modularity of the preparation approach. The available space for absorbates can be engineered in the shape of nanochannels lined with an infinite number of receptors for targeted and selective physisorption. Selectivity is provided not only by the channel opening as in conventional zeolites but also by organic groups that focus specific interactions on the channel core and fabricate supramolecular structures that cooperatively stabilize gases that diffuse in. Originally studied by Allcock,[17] tris(*o*-phenylenedioxy)cyclotriphosphazene (TPP, **1**) has become a compound of choice to investigate the structural features of organic zeolites and their potential applications. Studies have focused on the stability of the hexagonal modification compared to compact guest-free monoclinic structures:[18] single-crystal X-ray determination of the crystal structure,[19] investigation of gas storage or aromatic guest insertion by advanced NMR techniques[20] and X-ray diffraction,[21] confinement of iodine molecules by several crystallization procedures,[22] insertion of dipolar molecules,[23] obtainment of functional materials by inclusion of electroactive molecules,[24] and formation of nanocomposites containing macromolecules.[25] From TPP to some of its derivatives it has been shown that the available space for absorbates can be modulated by the choice of the side group, which substitutes the dioxyphenylene in the former, the key factor of tunnel formation being reported to be the rigid "paddle wheel" molecular shape and requirements of the crystal state.[26] For example, it was reported that TPP and tris(2,3-dioxynaphthyl)cyclotriphosphazene (TNP, **3**) spontaneously form inclusion adducts with benzene, toluene, heptane, octanes, and many other compounds,[17,27] whereas tris(2,2′-dioxybiphenyl)cyclotriphosphazene (**2**) forms no inclusion adducts when crystallized from or brought into contact with organic liquids. Furthermore, **3** is stable at least up to 350 °C, while **2** polymerizes above 250 °C.[27] These differences have been attributed to the greater molecular rigidity of **1** compared to **2** and the stabilizing influence of a seven-membered ring at phosphorus in the latter.[27] On the other hand, spontaneous inclusion adducts formation with **1** and a series of related derivatives was attributed to the "paddle wheel" molecular shape (associated to the requirements of the crystal packing). In the case of **1** and those derivatives clathration was characterized as a pure mechanical phenomenon.[28] Some of its relevant applica-

* To whom correspondence should be addressed. Phone: (+) 86-431-85099372. Fax: (+) 86-431-85684937. E-mail: zhangjingping66@yahoo.com.cn.
† Northeast Normal University.
‡ Université du Burundi.
§ CMS Institute of Chemistry.

10.1021/jp804185r CCC: $40.75
Published on Web 12/12/2008

tions however may be based on the physicochemical properties of these kinds of materials. Within TPP OZ, for example, which shows a strong affinity to include gaseous methane, carbon dioxide,[19] iodine,[22,25] and xenon,[20c] specific host−guest interactions of the donor−acceptor type were expected for channels.[19] Thus, the stability of the inclusion compound $TPP(I_2)_{0.75}$ up to temperatures as high as about 420 K[22] was interpreted based on the Lewis acidity of iodine and the electron-donor (E-D) capacity of the TPP−phenylenedioxy rings.[22] Although a number of theoretical investigations on phosphazene-containing systems can be found in the literature,[29−33] very few were devoted to phosphazene-based organic zeolite. Thus far a number of TPP derivatives have been experimentally isolated by extending the phenylenedioxy from one to three phenyl rings[17,27,28b,34] and through a partial or total O/NH substitution.[35] With **2** a set of interesting (structural) features was experimentally investigated.[28b] Among these, a comparison in bond lengths, bond angles, and phosphazene ring conformation with related cyclophosphazene was made to obtain some insight into the influence of the bulky dioxybiphenyl unit on the bonding within the phosphazene skeleton and a structural explanation of the chemical differences between **1** and **2**.[28b] No such study was found in the literature about other already isolated derivatives, and to the best of our knowledge, no CH/N derivatives have been reported. Even for the already isolated derivatives (**3**−**5**) many of their properties are still unknown.

In our previous reports[36,37] both ab initio and density functional theory (DFT) approaches were used with the aim of searching for a more accurate method for prediction of the molecular structure of TPP. Although a reliable model was found based on a hybrid-generalized gradient approximation (GGA) method, careful analysis of the optimized geometry showed that, at a certain degree, a more accurate model is still needed for such a molecule whose geometry is known as being key to tunnel formation on which its utility as zeolite is based. In this study more accurate methods are used to examine the effect of the CH/N heterosubstitution on a set of properties including the "paddle wheel" molecular shape, the structural stability upon charge injection, and the E-D capacity and thus electronic structure, which seemingly make TPP a good material for OZ use. In addition, we also discuss its influence on the length of the side fragment on which the available space for absorbates depends. In this way, we hope to contribute to a good understanding of the chemical and physical properties of such a growing family of materials while at the same time attempting to design new candidates.

2. Computational Methods

All single molecular geometry optimizations for the neutral and ionic forms were performed using the BH&HLYP half and half functional (where the HF exchange contribution amounts to 50%)[38] with the 6-31G(d,p)[39−42] basis set. Hartree−Fock (HF) theory was combined with the 6-311+G(d) basis set being applied in a single-point calculation to predict the orbital energies. The neutral form was optimized within C_3 symmetry and the cation without any symmetry constrains (C_1). The calculated harmonic vibrational frequencies did not reveal any imaginary frequency. Using the optimized geometries single-point energy calculation was carried out at a higher level with the aid of the same functional coupled to 6-311+G(d)[43−45] to improve the accuracy in energy. The first ionization potential (IP) was then calculated as described in the following equations

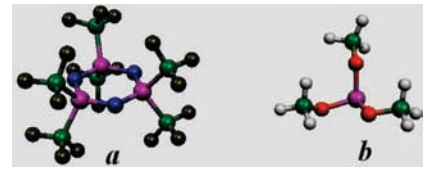

Figure 1. BH&LYP/6-31G(d)-optimized structures for $[NPCF_3]_3$ (a) and P-$(OMe)_3$ (b), where phosphorus, oxygen, nitrogen, carbon, fluorine, and hydrogen are shown in pink, red, blue, green, gray, and white, respectively.

$$IP = E_M^{+} - E_M^{0} \quad (1)$$

$$IP = -E_{HOMO} \quad (2)$$

where E_M^{+} and E_M^{0} are the total energies of the neutral and cationic forms, E_{HOMO} being the energy of the highest occupied molecular orbital (HOMO) at the optimized molecular structure in the neutral form according to Koopmans' theorem.[46] All computational studies were performed with the GAUSSIAN 03[47] series of programs with density functional methods as implemented in the computational package. The optimized geometries and molecular orbitals were plotted using MOLEKEL, 4.3 version,[48] and the density of states (DOS) calculated and convoluted using Pymolyze 2.0.[49] Computational studies on the packing structures were performed using the module Discover of the software package Materials Studio 4.0[50] and the compass force field parametrized for phosphazenes. [51]

3. Results and Discussion

3.1. Choice of the Computational Methods. A preliminary study based on different DFT approaches used to predict the TPP and TPP-like molecular structures showed that P═N and P−O bonds are very sensitive to the DFT approach applied (see Table S1, Supporting Information). While the meta-GGA do not offer any significant accuracy improvement with respect to the GGA approaches, both providing too large deviations from experimental structures, more accurate results were obtained with hybrid-GGA, where the percent of HF exchange rules the quantitative results, especially for the P−O bond. It was found that the hybrids including 50% of HF exchange (BH&H/BH&HLYP)[38] are the most accurate, whereas B3PW91[52] and PBE0[53] also provide relatively good estimates (see Table S1, Supporting Information). For comparison and calibration, since no gas-phase electron diffraction (GED) structure is available yet for TPP, $[NPCF_3]_3$ and P−$(OMe)_3$ bearing P═N and P−O bonds (Figure 1a and 1b) were calculated with the same methods and compared to their GED structures.[54,55] An excellent agreement was found with BH&HLYP structures (see Table S2, Supporting Information).

To evaluate the structural stability of this class of growing interest against charge injection it was found that HF leads to spin-contaminated results (see Table S3, Supporting Information). Although BH&HLYP was proven to be a robust method in prediction of the structures for neutral species, a certain spin contamination was also detected and, compared to the PBE0 and B3PW91 results, it was thought that BH&HLYP may not be suitable for ionic species in the case of TPP and TPP-like derivatives.

The E-D strength of the phenyl ring within TPP affects the stability of the adsorbent···adsorbate complex.[22] Recently, we demonstrated a tight relation between the IP of TPP-like molecules and that of the free side fragment.[37] Then, one may directly estimate the effect of CH/N heterosubstitution on the E-D capacity of the side fragment from the IP of the entire

TABLE 1: Computed Ionization Potential (IP) along with Available Experimental Data for the Phosphazene Derivatives of Reference[a]

molecule	IPv	IPa	Calcd[d]	exp[d]
$P_3N_3F_5OCH{=}CH_2$	10.08,[b] 10.09[c]	9.35[c]	10.79	10.61
$P_3N_3F_4(OCH{=}CH_2)_2$	9.27,[b] 9.30[c]	8.89[c]	10.37	10.09
$P_3N_3F_5C_6H_5$			10.04	10.07
2,2-$P_3N_3F_4(C_6H_5)_2$			9.52	9.64
cis-2,4-$P_3N_3F_4(C_6H_5)_2$			9.81	9.62
trans-2,4-$P_3N_3F_4(C_6H_5)_2$			9.76	9.62

[a] IPv and IPa represent the vertical and adiabatic ionization potentials, respectively. [b] From eq 1 at the B3LYP/6-311+G* level. [c] From eq 1 at the PBE0/6-311+G* level. [d] From eq 2 at the HF/6-311+G(d) level. [d] From ref 56.

molecule. Preliminary calculations have proved that based on Koopmans' theory[46] HF/6-311+G* can yield an excellent accuracy for adiabatic IP (see Table S4, Supporting Information). Again, since no experimental IP value for TPP is available yet, a number of molecules with nearly the same atomic composition whose experimental IP values are already available were selected.

Those include $P_3N_3F_5OCH{=}CH_2$, $P_3N_3F_4(OCH{=}CH_2)_2$, $P_3N_3F_5C_6H_5$, 2,2-$P_3N_3F_4(C_6H_5)_2$, *cis*-2,4-$P_3N_3F_4(C_6H_5)_2$, and *trans*-2,4-$P_3N_3F_4(C_6H_5)_2$ studied by C. W. Allen et al.[56] As shown in Table 1 very good accuracy was also found between our predicted IP values and the experimental adiabatic first-ionization potentials[56] for a number of substituted phosphazenes considered as references in this work. Consequently, more reliable structures for neutral species, estimates of the structural stability upon charge injection, and IP evolution in the new TPP derivatives of interest in this study can be reasonably awaited from the BH&HLYP/6-31G(d,p), PBE0/6-31G(d,p), and HF/6-311+G(d) levels, respectively.

3.2. Neutral Species. ***3.2.1. Molecular Features.*** *TPP and TPP-like with Enhanced π Conjugation.* We begin our discussion with the already synthesized compounds (**1**−**5**) which correspond to extending the phenylenedioxyl side group (within TPP) with one or two more phenyl rings, linearly or laterally. In Scheme 1 we show the chemical structures corresponding to a different arrangement of the two or three rings in one side fragment. Some of the corresponding optimized structures are displayed in Figure 2, and selected parameters are listed in Tables 2 and S4, in the Supporting Information (which also show available experimental data for comparison). Since experimental observations favor C_2 symmetry for **2**, geometry optimization within this symmetry was also considered besides the C_3 one. From the optimized geometries the common and most important feature was found to be the planarity of the cyclophosphazene ring, in agreement with an experimental report, except for **2** for which a slight deviation from the planarity of the phosphazene ring (by ∼3°) was predicted for C_2, in agreement with an experimental report.[15] According to the BH&HLYP/6-31G(d,p) results the C_3 conformation (−3024.998714 au) was found to be the preferred form of **2**, being energetically more stable than the C_2 one (−3024.9969577 au) by ∼1.1 kcal, in agreement with our previous report based on different levels of theory.[37] This feature also agrees with an experimental report by Allcock et al.[28b] according to which conformations other than the experimentally observed C_2 may be awaited in solution or the molten state since the later was demonstrated as mainly resulting from crystal packing forces. Also in agreement with experimental observations is the planarity of the side fragment in the case of **1**, **3**, and **5** and, of course, the twisted heterocycle (containing the two O atoms) in **4**.

SCHEME 1: Chemical Structures of the Derivatives under Investigation[a]

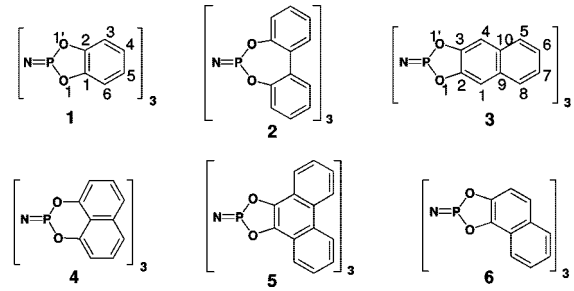

Pristine [a]	n [b]	Side fragment	Dvt.[c]
		Cyclohexatrienediol-1,2	**1**
	3	Pyridine-2,3-diol	**7**
	4	Pyridine-3,4-diol	**8**
TPP	3 & 6	Pyrazine-2,3-diol	**9**
	4 & 5	Pyridazine-4,5-diol	**10**
	3 & 5	Pyrimidine-4,5-diol	**11**
	3 & 4	Pyrimidine-3,4-diol	**12**
		Naphthalene-2,3-diol	**3**
	1	Quinoline-2,3-diol	**13**
	5	Quinoline-6,7-diol	**14**
	6	Isoquinoline-6,7-diol	**15**
	1 & 4	Quinoxaline-3,4-diol	**16**
	5 & 8	Quinoxaline-6,7-diol	**17**
TNP	6 & 7	Phthalazine-6,7-diol	**18**
	1 & 8	[1,5]Naphthyridine-2,3-diol	**19**
	1 & 7	[1,6]Naphthyridine-2,3-diol	**20**
	1 & 5	[1,8]Naphthyridine-2,3-diol	**21**
	1 & 6	[1,7]Naphthyridine-2,3-diol	**22**
	5 & 6	Cinnoline-6,7-diol	**23**

[a] Only **1**−**5** have been synthesized and clathration evidenced for **1** and **3**−**5**.[17,26,28,34] The numbering scheme used in the text for the atoms in the side group is also shown. [b] The positions for systematic substitution of CH groups with N atoms. [c] TPP, TNP, and their derivatives.

Despite the use of 6-31G(d,p), which includes the d polarization functions known to be necessary for an accurate description of the chemistry of phosphorus[36] and the BH&HLYP that takes into account the electron correlation proved to be necessary for proper description in the case of TPP, some of the optimized (geometrical) parameters for **2** significantly deviates from the reported crystal structure (geometrical not given in this contribution).[27] This can be reasonably ascribed to the reported fact that the molecular geometry of **2** suffers from the solid-state effects in its crystal.[27] In general, this may be taken as being in agreement with experimental observation. Again, these features give credit to the BH&HLYP/6-31G(d,p) chemical model to predict the geometrical structures of this kind of systems.

CH/N-Substituted Derivatives. With the aim of evaluating the influence of CH/N heterosubstitution on the molecular structure of TPP and TPP-like molecules, compounds **1** and **2** were considered for this issue. The molecular models used in our calculations, obtained by a systematic substitution of CH groups with N atoms in positions 3, 6, 4, and/or 5 for **1** on one

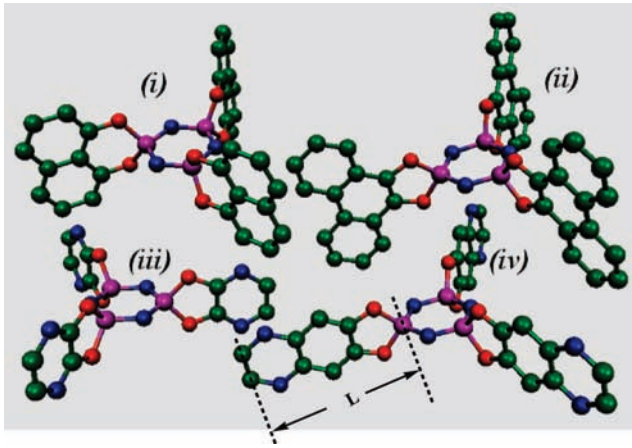

Figure 2. BH&HLYP/6-31G(d,p)-optimized structures for (i) **4**, (ii) **5**, (iii) **9**, and (iv) **17** as representatives of the series of compounds under investigation (for clarity, hydrogen atoms are not shown).

hand and 1, 4, 5, 8, 6, and/or 7 for **2** on the other hand, are shown in Scheme 1. In the following the results are presented according to the labeling method adopted in the same scheme. From the optimized geometries of this series of derivatives (**7**−**24**) the common feature was found to be preservation of the "paddle wheel" molecular shape with longer side fragments for TNP derivatives than for TPP derivatives.

Again, it was found that the geometrical parameters involving the phosphazene ring remain practically unaffected. Indeed, no more than 0.007 Å (0.018 Å) in N−P (P−O) bond lengths of deviation is predicted, while less than 2° of deviation was revealed from N−P−N, P−N−P, and O−P−O bond angles. These results are shown in Table 2 for representatives (**9**, **14**, **16**, and **17**) of this kind of series. From the length of the side fragment viewpoint, on which depends the available space for adsorbates, we anticipate a decreasing diameter of the tunnel with the degree of CH/N substitution within both TPP and TNP. This can be explained by comparing the C−C bond length of the unsubstituted bond (1.37−1.41 Å) to that of the corresponding C−N one (1.28−1.30 Å) in the CH/N-substituted derivatives. On the basis of our results the magnitude of the variation is expected in the decreasing order unsubsituted > monosubstituted derivatives > disustituted derivatives. Thus, the size of the adsorbing space in CH/N derivatives of TPP may be anticipated to be smaller than that of TPP itself, while CH/N derivatives of TNP would lead to crystals having a tunnel space in between those with TPP and TNP. Compared to the TPP molecular shape CH/N substitution breaks the D_{3h} symmetry in the case of the monosubstituted and disubstituted derivatives other than **11**, **12**, and **19**−**24** while inducing a uniform change on the P−O bond length which is found to be slightly shortened (≤0.007 Å) on one side and remarkably lengthened (up to 0.015 Å) on the other side of the side fragment. It is interesting to note that in all CH/N derivatives no more than 0.02 Å of change is predicted in bond length, the greatest deviation in bond angle being found to be less than 2°, the planarity of the side group and its perpendicularity to the plane of the central ring being preserved.

3.2.2. Electronic Structure. *Charge Partitioning within the Phosphazene Ring.* The Mulliken partial atomic charges for the central (and common) part to all of the molecules under investigation are summarized in Table 3. From these one can find that the nitrogen atom accumulates an excess of negative charge (ca. −0.65 e^-), the phosphorus atoms being highly positively charged (∼1.20 e^-), resulting in a highly polarized P−N bond in contrast to the P−O one involving two negatively charged P and O atoms. This feature agrees well with the previous ab initio theoretical report by Waltman et al.[32] on a series of cyclophosphazenes and is observed to remain in the two kinds of derivatives envisaged in this study.

Frontier Molecular Orbitals (FMO) Shape. Analysis of the molecular orbitals can provide very useful information about a molecule, such as the site of electron attachment and detachment as well as chemical reactivity.[57] Moreover, in HF calculation it is possible to obtain the IP from Koopmans' theorem, which has proven to be highly accurate for cyclophosphazenes (see Table 1). In return, DFT has been widely used because the accuracy of the energy of the energy calculation is normally higher than that of HF. Therefore, the accuracy of the DFT-optimized structures is also higher than the HF-based one. In this work both HF and DFT were applied to probe the electronic structures of the system of interest. In Figure 3 we show the HOMOs of **1**, **9**, **16**, and **17** as representative of the series of derivatives under study. First, it is interesting to note how well the distribution of the HOMOs for $P_3N_3F_5OCH{=}CH_2$ and $P_3N_3F_4(OCH{=}CH_2)_2$ correlates with the assumptions based on the experimental observations by C. W. Allen et al., who assigned the first vertical IPs for $P_3N_3F_5OCH{=}CH_2$ (10.61 eV) and $P_3N_3F_4(OCH{=}CH_2)_2$ (10.09 eV) to the phosphazene out-of-plane π-orbital ionizations, leaving them as being derived from the $O{-}CH{=}CH_2$ moiety, in agreement with previous observations of the general range of energies associated with this functional group.[56] This assignment is confirmed by the HOMOs π nature and distribution on $O{-}CH{=}CH_2$ as computed and shown in Figure 3 (i and ii). This good agreement also gives credit to the conclusions to be drawn from the same viewpoint in the case of the systems under investigation.

From Figure 3 one may observe that for the representatives of the systems under study the HOMO is uniformly and strongly localized on the three side fragments, the LUMO (not shown here) being mainly made of contributions from two of the three side groups. In addition, one may find that the former is binding on $C_2{-}C_3$, $C_6{-}C_7$, and $C_9{-}C_{10}$ bonds for TNP and its derivatives ($C_1{-}C_2$ and $C_4{-}C_5$ for TPP) while antibonding between the O and the adjacent carbon atoms. The same features were previously described for the TPP molecule parent based on different wave functions. [37]

In the whole series of new derivatives the HOMO shows almost the same bonding−antibonding pattern; it is localized on the residual phenylenedioxyl side (mainly on O_1, $O_{1'}$, C_1, C_2, C_4, C_5, and/or the substituting N atom) and uniformly (or almost) localized on the three side groups. The LUMO also shows common characteristics in the whole series: it is localized on the residual side moiety with significant contribution from the nitrogen in some of the derivatives and a negligible contribution from O atoms. In addition, as for the pristine TPP it is strongly and uniformly localized on two of the three side groups with a weak contribution from the remaining other. From these features we anticipate and confidently assign the first vertical IP of the phosphazenes under study to the phosphazene out-of-plane π-orbital ionizations, leaving them as being derived from the side moieties.

Frontier Molecular Orbitals Energies (E_{FMO}). The HOMO belongs to the irreducible representation ***A*** with an eigen value (E_{HOMO}) of −8.97 eV, whereas the HOMO-1 and HOMO-2 are ***E*** with an eigen value ($E_{HOMO\text{-}1}$ and $E_{HOMO\text{-}2}$ degeneracy case) equal to − 9.07 eV. It is interesting to note how well the HF/6-311+G(d) values agree with the HF/6-31G**//PBE0/6-31G** ones of −8.79 and −8.89 eV, respectively, from our previous

TABLE 2: Selected BH&HLYP/6-31G(d,p)-Optimized Bond Lengths (*R*, Angstroms) and Bond Angles (*θ*, degrees) for TPP and Some of Its Derivatives (both the *π*-extended and CH/N-substituted derivatives)[a]

	1	**3**	**5**	**6**	**9**	**14**	**16**	**17**
N−P	1.579	1.578	1.579	1.579	1.576	1.578	1.576	1.578
P−O_1	1.622	1.621	1.623	1.622	1.626	1.622	1.624	1.621
P−$O_{1'}$	1.622	1.620	1.623	1.623	1.626	1.620	1.624	1.621
C_1−O_1	1.374	1.372	1.377	1.376	1.363	1.371	1.363	1.369
$C_{1'}$−$O_{1'}$	1.374	1.372	1.377	1.376	1.363	1.371	1.363	1.369
$C_{1'}$−C_1	1.383	1.407	1.341	1.359	1.396	1.408	1.423	1.410
N−P−N	116.4	116.4	116.3	116.3	116.6	116.4	116.7	116.5
P−N−P	123.6	123.6	123.7	123.7	123.4	123.6	123.3	123.5
P−O_1−C_1	110.4	110.9	109.5	110.0	110.3	110.9	110.9	111.1
P−$O_{1'}$−$C_{1'}$	110.4	110.9	109.5	109.8	110.3	111.1	110.9	111.1
O_1−C_1−C_1'	111.8	111.3	112.7	112.2	111.9	111.3	111.2	111.2
$O_{1'}$−$C_{1'}$−C_1	111.8	111.3	112.7	112.4	111.9	111.1	111.2	111.2
O−P−O	95.6	95.7	95.5	95.6	95.7	95.6	95.8	95.5

[a] See Scheme 1 for atom definition.

TABLE 3: BH&HLYP/6-31G(d,p) Mulliken Charge Distribution Representative of the Series of Compounds under Study (1, 3, 5, 6, 9, 14, 16, and 17)

a	**1**	**3**	**5**	**6**	**9**	**14**	**16**	**17**
P	1.231	1.230	1.231	1.231	1.231	1.231	1.237	1.232
N	−0.665	−0.630	−0.664	−0.665	−0.655	−0.661	−0.654	−0.659
O_1	−0.622	−0.625	−0.637	−0.624	−0.595	−0.621	−0.597	−0.659
$O_{1'}$	−0.622	−0.625	−0.637	−0.634	−0.595	−0.624	−0.597	−0.620

[a] See Scheme 1 for atom definition.

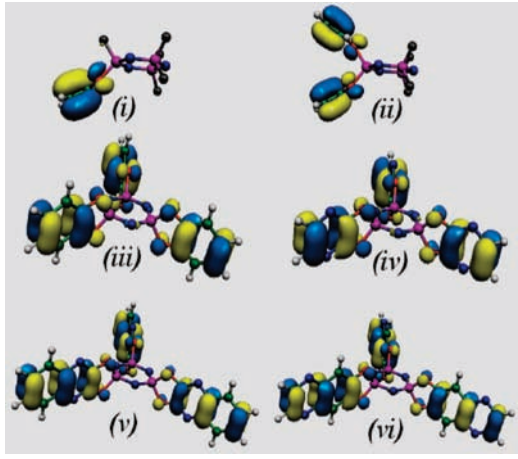

Figure 3. BH&HLYP/6-31G(d,p) HOMOs for (i) $P_3N_3F_5OCH{=}CH_2$, (ii) $P_3N_3F_4(OCH{=}CH_2)_2$, (iii) **1**, (iv) **9**, (v) **16**, and (vi) **17** as representatives of the series of derivatives under investigation.

work,[37] implying the nearly same accuracy in the predicted structure of the neutral species. In agreement with those provided using the 6-31G(d,p) and 6-311G+(d) basis sets, the energy splitting is predicted to be ca. 0.1 eV between the highest and next highest occupied levels. These features clearly indicate that the E_{FMO} energies ordering and related qualitative features may not be very affected by the basis set or electronic wave function, implying the reliability of the results. In Table 4 we only list the calculated energies for the E_{HOMO} and E_{LUMO} eigenvalues for the investigated compounds relative to pristine TPP and TNP as obtained from BH&HLYP/6-31G(d,p) and those computed with HF/6-311+G(d) at the BH&HLYP/6-31G(d,p)-optimized structures. Those related to compounds **4**−**6** are also listed for the sake of comparison. From the results presented in Table 4 a general trend that is observed is that the *π*-conjugation length increases the E_{HOMO} while decreasing the E_{LUMO} in the sequence **1** < **3** < **4** < **6** < **5**. In contrast, the CH/N substitution in the side fragment decreases (and stabilizes) the HOMO and LUMO eigenvalues at the same time owing to the presence of one/two

TABLE 4: Calculated Length (*L*) of the Side Fragment, HOMO Energy (E_{HOMO}), LUMO Energy (E_{LUMO}), and HOMO−LUMO Gap (E_g)[a]

	BH&HLYP/6-31(d,p)				HF/6-311+G(d)		
	L^b	E_H	E_L	E_g	E_H (−IP_{KT})[c]	E_L	E_g
1	4.72	−7.50	0.99	8.49	−8.97	1.53	10.50
3	7.16	−6.99	0.05	7.04	−8.20	1.57	9.77
4	5.03	−6.71	0.09	6.80	−7.88	1.55	9.42
5	5.91	−6.47	0.07	6.54	−7.71	1.53	9.24
6	5.95	−6.69	0.01	6.69	−7.92	1.55	9.47
7	4.64	−7.91	0.30	8.21	−9.34	1.39	10.73
8	4.70	−8.31	0.42	8.73	−9.80	1.33	11.13
9	4.56	−8.40	−0.48	7.92	−9.80	1.40	11.20
10	4.70	−8.77	−0.35	8.42	−10.94	1.07	12.01
11	4.62	−8.81	−0.23	8.58	−10.33	1.28	11.61
12	4.63	−8.98	−0.50	8.48	−10.64	1.09	11.72
13	7.07	−7.53	−0.35	7.18	−8.81	1.45	10.26
14	7.07	−7.56	−0.36	7.20	−8.84	1.46	10.30
15	7.13	−7.48	−0.45	7.03	−8.68	1.34	10.02
16	6.98	−7.98	−0.86	7.12	−9.21	1.32	10.53
17	6.99	−7.91	−0.90	7.02	−9.11	1.17	10.28
18	7.12	−8.31	−0.90	7.42	−9.62	1.02	10.64
19	7.05	−7.93	−0.74	7.19	−9.16	1.37	10.53
20	7.04	−7.96	−0.84	7.12	−9.20	1.24	10.44
21	6.98	−7.93	−0.74	7.18	−9.15	1.29	10.44
22	7.04	−8.03	−0.87	7.16	−9.24	1.18	10.43
23	7.05	−8.04	−1.02	7.02	−9.30	1.16	10.45
24	7.05	−8.05	−0.86	7.19	−9.29	1.25	10.54

[a] $E_H = E_{HOMO}$ and $E_L = E_{LUMO}$. [b] *L* is calculated as described in Figure 2. [c] Ionization potential (IP_{KT}) is estimated using eq 2.

nitrogen atom(s) and very dependently on the position of the substituted CH group in the side fragment. Due to the inductive effect of the nitrogen atom, the HOMO gets stabilized in the sequence **1** < **7** < **8** < **9** < **10** < **11** < **12** within the subgroup of TPP and its CH/N derivatives and in the sequence of **3** < **15** < **13** < **14** < **19** < **21** < **19** < **20** < **16** < **22** < **23** < **24** < **18** in the subclass of TNP and its CH/N derivatives. It is interesting to note that both the HOMO and LUMO are more stabilized in the disubstituted ones (**10**−**12** for the TPP based and **17**−**20**

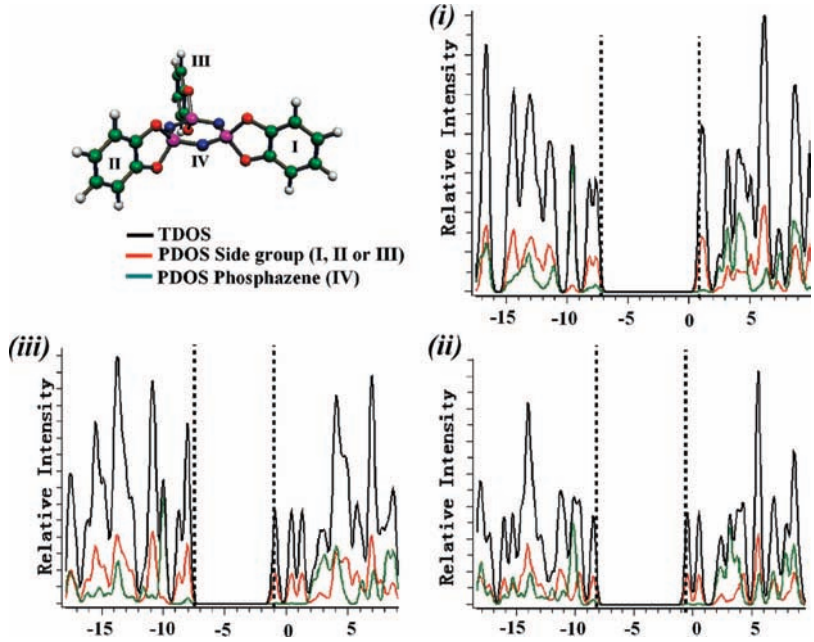

Figure 4. Total and partial density of states (TDOS and PDOS) around the HOMO−LUMO gap for (i) **1**, (ii) **9**, and (iii) **17** as computed at the BH&HLYP/6-31G(d,p) level of theory (dashed vertical lines indicate the HOMO and LUMO energies).

for the TNP based) than the monosubstituted derivatives owing to the one more N atom in the former cases. Relative to TPP, the greatest increase in E_{HOMO} (1.26 eV with the HF and 1.03 eV with the BH&HLYP) was observed for **5**, the greatest decrease of ∼2.00 eV with the HF, and ∼1.27 eV with the BH&HLYP being predicted for **10**. The predicted net effect was that, in comparison to TPP, the HOMO−LUMO gap energy within the BH&HLYP results remarkably decreases for **3**−**6**, and **13**−**24**. These results agree well with the HF-based ones except for compounds **7**−**12**, **16**, **18**, **19**, and **24**, whose E_g values appear to be slightly greater than that of **1**. Compared to TPP, extending the side group with an aromatic ring destabilizes the HOMO, which becomes more stabilized by CH/N substitution.

Total and Partial Density of States (TDOS and PDOS) around the HOMO−LUMO. The electronic structures should represent the fingerprints of the organic molecule in relation to the chemical and physical properties.[58] Although ultraviolet photoemission spectroscopic (UPS) measurements can provide such information, there is still a lack of accuracy in the detailed information relating to individual atoms involved.[59] In our previous studies on TPP[36,37] some insight was gained on the electronic structure of the molecule through a brief analysis of the FMOs. To supplement these studies, on the way to a detailed comparative study of the effect of the π-conjugation length and CH/N substitution on the electronic structure for the molecules under investigation, the TDOS and PDOS on four fragments were calculated based on the current level of theory. The results are plotted for three representatives of derivatives (**1**, **9**, and **17**) and shown in Figure 4. As clearly shown in this figure, the PDOS reveals that the HOMOs are fairly localized on the phosphazene ring with only minor but nonzero contributions from its nitrogen atoms, the main contributions coming from the side fragments. In the same figure one can find that the LUMOs are highly delocalized throughout the ring(s) of the side fragment with no contributions from the oxygen atoms and the phosphazene moiety. One of the advantages of DOS study is that identification of any other molecular orbitals can also be made in a straightforward way. By examining the PDOS it was found that O_1, C_1, C_3, and C_4 have symmetrical contributions to those for $O_{1'}$, C_2, C_6, and C_5. This implies the existence of a σ_h plan, which in the case of TPP coincides with the plan of the central ring, in agreement with the D_{3h} symmetry from experimental observation.[33] The same feature was observed with TNP and might be also revealed in CH/N-disubstituted derivatives **16**−**18**.

Although UPS measurement can provide similar (maybe more accurate) valence band information, projection of TDOS to individual atoms explicitly reveals the contributions to TDOS from each atom which are not possible from the UPS measurement. Information regarding the reactive and excitation points in the TPP and some of its derivatives can also be obtained from Figure 3. The atoms associated with the HOMO are likely to give up electrons upon reduction. Those atoms (O, C, and N in case of some CH/N-substituted derivatives) contributing more to the HOMO are more likely to react with other atoms and may be responsible for the reactivity of the molecules, including the donor−acceptor behavior when a Lewis acid (such as I_2 within TPP crystals) is adsorbed. Although no UPS measurement related to the studied cases were found in the literature, the consistency of the HF-based TDOS and PDOS with the PBE0 (see ref 37) and the BH&HLYP-based ones imply a certain reliability of the present treatment, while new information such as reactive and excitation sites in the molecule and electronic localization properties revealed in this work would lead to a better understanding of the molecular properties of TPP-like and the corresponding CH/N-substituted derivatives.

3.3. Cationic Forms and Ionization Potential. To investigate the effects of charge injection on the molecular conformational stability the structural and electronic properties of the cation have been calculated. For this purpose, geometry optimization was carried out on the cationic form (i.e., the neutral molecule in the presence of an extra hole). In Table 5 we show the predicted structural changes for **7** and **9** (chosen as representatives for this study) compared to their neutral forms. Only parameters involving the side fragments are displayed since in both two cases the phosphazene ring was found to remain unaffected by charge injection. As previously found and reported for TPP[36] and some other derivatives[37] loss of symmetry upon

TABLE 5: Selected Calculated Variation of Structural Parameters in the Cation for Derivatives 7 (monosubstituted) and 9 (disubstituted) Compared with Their Neutral Forms[a]

ΔR (Å)[b]	7	9	$\Delta\theta$ (deg)[c]	7	9
$P-O_1$	0.003	0.005	$P-O_1-C_1$	0.42	0.32
$P-O_{1'}$	0.005	0.006	$P-O_{1'}-C_2$	0.42	0.32
O_1-C_1	−0.013	−0.013	$O_1-C_1-C_2$	−0.13	−0.07
$O_{1'}-C_2$	−0.013	−0.013	$O_{1'}-C_2-C_1$	−0.20	−0.07
C_1-C_2	0.014	0.011	$O_1-P-O_{1'}$	−0.52	−0.49
C_1-C_6	0.000	0.004	$C_2-C_1-C_6$	0.03	0.06
C_2-C_3	0.006	0.004	$C_1-C_2-C_3$	0.21	0.06
C_3-C_4	−0.007	−0.010	$C_1-C_6-C_5$	−0.31	−0.22
C_6-C_5	−0.008	−0.009	$C_2-C_3-C_4$	−0.56	−0.22
C_5-C_4	0.017	0.022	$C_6-C_5-C_4$	0.19	0.16
			$C_3-C_4-C_5$	0.42	0.16

[a] See Scheme 1 for atom definition. [b] ΔR = variation in bond length. [c] $\Delta\theta$ = variation in bond angle.

charge injection was found to be so minor that the calculated geometrical differences for the residual three side fragments were negligibly small. The results listed are those relative to one of the three side fragments but reflect the behavior of the other two. In these the negative and positive values express, respectively, the increase and decrease of the parameters of interest. For each spirocyclic side group both the bond lengths and the bond angles change symmetrically except for the monosubstituted derivatives. Changes in bond lengths are not significant (at most 0.013 Å for **7** and 0.022 Å for **9**), those in the bond angles being found to be less than 1°. Changes in bond lengths are mainly localized in the bridging part containing the C−O bonds whose lengths decrease. Upon depopulating the redox-active molecular orbitals the C_1-C_2 and C_4-C_5 bonds are lengthened and the C−O bonds adjacent to the former shortened. It is important to note that these features, based on PBE0, are nicely reflected in the BH&HLYP-calculated HOMOs (Figure 3), which are bonding on C_1-C_2 and C_4-C_5 while antibonding between the former and the O atoms.

On the basis of the relatively small structural relaxation upon injection of positive charge, as revealed by the current calculations, a certain structural stability, especially versus a positive charge injection, might be expected from these derivatives. Assuming that the corresponding crystal requirements responsible for tunnel formation can be attained, this may make them tolerant hosts for guest molecules of Lewis acid character, as the pristine TPP. On applying Koopmans' theorem (eq 2) the IP values were computed at the HF/6-311+G(d) level on the BH&HLYP/6-31(d,p) geometries. It is noteworthy to recall the excellent agreement between experimental and computed IP for phosphazene. Since then the E-D capacity of the series of compounds studied which can be reliably measured from the IP is expected to be more accurate than what one could expect from the energy difference (eq 1) based on the commonly used DFT approaches. Indeed, whereas sufficiently good qualitative conclusions can be drawn from the IPs computed from these, we found that applying Koopmans' theorem at the HF/6-311+G(d) level in the cases of c and d (see Table 1) leads to more accurate results for phosphazenes. As listed in Table 4, the results clearly show that the energy required to create a hole in TPP, i.e., 8.97 eV, is much higher than both adiabatic (and vertical) values of ca. 7.53 (7.60)[36] and 7.63 eV (7.70 eV)[37] based on the B3LYP and BPE0 methods, respectively. Careful analysis of the computed IP values listed in Table 4 shows that the π-conjugation length within TPP considerably decreases the IP, which significantly increases upon CH/N substitution. Confirming some other findings recently reported elsewhere[37] the IP values reveal that the E-D capacity of TPP side groups is tunable, allowing predictions to be made about the stability of the inclusion compounds of OZ and molecules of Lewis acidity comparable to that of I_2. Herein, the results confirm that π-conjugation length decreases the IP in the sequence **1** < **3** < **4** < **6** < **5**. A comparison of **3**, **4**, and **6** shows again that the IP is even decreased by a lateral extension. The E-D strength is then increased within the same order. The stability of the inclusion compound, $TPP(I_2)_x$, and the operating temperatures may then be improved using **3** and **4** whose clathrates with many other molecules (such as benzene,[17] xylenes,[60] etc.) are already known, with the OZ−I_2 inclusion compound based on **3** being expected to be less stable than that based on **4**. This stability is expected to be reduced within CH/N-monosubstituted derivatives and even more reduced in disubstituted. This feature is important since it provides a way to control the adsorbate according to the desired application. Another interesting feature that can be derived from this study is shortening of the length of the side fragment, which was reported and expected to affect the available space for the adsorbates, allowing the amount of the later to be modulated. From these results, if again we assume that crystal requirements (not treated in this work) can be attained, clathrates of good tolerance (toward guest molecules in a wide range of Lewis acidity) within a wide range of E-D capacity and available adsorbates space may be awaited from CH/N substitution within TPP-like molecules. On the basis of these properties some of the possible guests that can be awaited to be trapped in the crystals of the molecules studied (hosts) are at least the number of compounds with a Lewis acidity comparable to that of I_2 and smaller (in size) than xylene.

3.4. CH/N Substitution Effects on the Solid State. The crystal structure of **1** resembles the structure of **3** with some differences being reported.[17] From a structural viewpoint, the phosphazene ring in the former is perfectly planar (since both phosphorus and nitrogen lie on the mirror plane) and the plane of the phenylenedioxyphosphole unit oriented exactly at 90° to the phosphazene ring plane, whereas the naphthalene residue in **3** is not totally planar.[17] A minimum diameter in the range of 9−10 Å was reported for the channels found in the clathrate formed by **3** (see Figure 5), where six benzene "spheres" per unit cell can be close packed in the wider segments of each channel.[17] In **1** the minimum channel diameter is less than 5 Å with only one benzene molecule statistically occupying the channel volume within each unit cell.[18] The stability differences between the benzene clathrates of **1** and **3** almost certainly reflect the different channel diameters in the two structures.[17] Since benzene molecules apparently can tumble within the channels formed by **3** they can presumably escape from these channels more readily than from the narrower channels formed by **1**. These features clearly demonstrate the crucial role of the tunnel diameter in the stabilization of the clathration process. It then appears to be interesting to evaluate the influence of the CH/N substitution discussed above from the same point of view. Without pretending to predict the crystalline structure of the CH/N derivatives of interest in the current study the results presented in this section assume that some of the CH/N derivatives (if not all) may retain the $P2_1/n$ (before clathration) and $P6_3/m$ (upon clathration) space groups in the corresponding crystals as observed when the side group is extended from one to two phenyl rings (from **1**[18] to **3**[17]). Since single molecules of both **1** and **3** are of D_{3h} symmetry group, we judged it to be more reasonable to conduct this evaluation on a disubstituted derivative (**17**) of the same symmetry. The computational results described in this section were performed by the method and

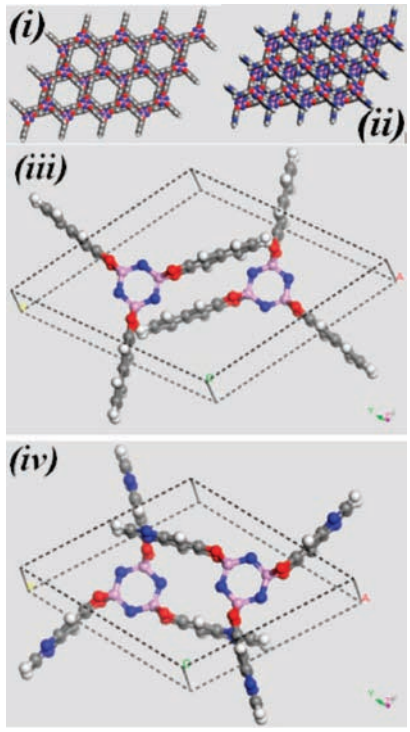

Figure 5. Hexagonal crystal packing of (i) **3** that forms channel-like structures with a 9−10 Å diameter, as reported by Allcock et al., (ii) **17** optimized channel-like structure with 7.91 Å diameter, and unit cells for (iii) **3** and (iv) **17**.

TABLE 6: Hexagonal Crystal Packing of (i) 3 That Forms Channel-like Structures with a 9−10 Å Diameter (as reported by Allcock et al.) and (ii) 17 (CH/N-disubstituted derivative)

parameter	**3**-$P2_1/n$[a]	**3**-$P6_3/m$[a]	**17**-$P6_3/m$
a (Å)	32.01 (−0.81%)	15.373 (−2.24%)	12.64
b (Å)	5.66 (−2.92%)		
c (Å)	27.16 (−1.31%)	10.011 (−0.65%)	10.96
β (deg)	96.82 (1.65%)		
D (Å)		9.46	7.37

[a] Percentages of deviations from experimental values from ref 17.

software described in the Computational Methods section. Validation of the force field was checked by optimizing the monoclinic packing and the empty TPP host structures of **1** and **3**. The host structures were derived from the TPP−benzene[13] and **3**−benzene[17] experimental structures. For **17** the structure used was derived from the latter by replacing the "CH" groups in positions 5 and 8 (see Scheme 1 for details) by N atoms and adjusting the geometrical parameters involved to the BH&HLYP/6-31G(d,p)-optimized ones for the single molecule.

The results are collected in Table 6. From the optimized structures for both **1** (previous work[33]) and **3** (in this work) one may figure out that the unit-cell parameters agree well with experimental data (maximum deviation of 5%) even though a tendency to obtain denser packing was observed. This indicates that the compass force field is suitable for describing not only **1**, in agreement with a previous report by Claire Gervais et al.,[33] but also **3**, which reinforces the credibility of the current results. From the tunnel size viewpoint the diameter (D) was estimated as described in the annex part provided in the Supporting Information. Again, it is interesting to note how good the agreement between the experimental (9−10 Å) and the predicted (9.30 Å) values is for **3** (also listed in Table 6). Confirming our anticipated conclusions from the predicted shortening of the side group upon CH/N substitution, that the size of the available space for adsorbates, the predicted D (= 7.91 Å) for the CH/N-disubstituted derivative (**17**) was found to be ∼1.4 Å smaller compared to that of the parent molecule **3**. Finally, careful analysis of the optimized structures of **3** and **17** as single molecules and crystals (unit cells) shows a more pronounced packing effect in **17**. Indeed, the snapshots in Figure 5iii and 5iv show that, initially planar in the single molecules, the side fragment would suffer from some slight bending effects for **3** which becomes even more obvious for **17** in the bridging part between the central ring and the first ring, leaving the rest of the side fragment planar (or nearly) and perpendicular to the plane of the phosphazene ring. This may suggest different intermolecular interactions in **17** compared to **3**, which does not mitigate against the main conclusion drawn from the current study about the influence of the CH/N substitution on the properties of TPP and TPP-like which make them good materials for organic zeolite use.

4. Conclusions

From this theoretical study some light was shed on the CH/N substitution along with enhancement of the π-conjugation effect on the zeolite TPP structures and properties: (i) BH&HLYP/6-31G(d,p) calculations indicated that CH/N substitution preserves the "paddle wheel" molecular shape, a key factor in tunnel formation on which the use of TPP and TPP-like molecules for OZ use is based. (ii) Both the HF/6-311+G(d) and BH&HLYP/6-31G(d,p) predictions are consistent with the HOMO and LUMO stabilization through CH/N substitution whose net impact can be either an increasing or a decreasing HOMO−LUMO gap depending on the position of the substituted CH group in the side fragment. (iii) On the basis of a comparative study between the PBE0/6-31G(d,p)-optimized structures for the neutral and cationic forms the CH/N-substituted derivatives were predicted to preserve the structural stability upon injection of a positive charge. (iv) On the basis of the calculated IPs a significantly large increase in the E-D capacity owing to the enhanced π conjugation through linear or lateral extension with an aromatic ring. Again, we showed that lateral extension induces the most significant E-D capacity. The features revealed by the current study indicate that the E-D capacity of TPP can be easily tuned by both the CH/N heterosubstitution and the lateral or linear extension of the side group with one or two aromatic rings on the side group. This may provide a way to modulate the stability of some guest···host complexes (by varying the E-D strength of the side group) and the amount/size of the adsorbate (through the length variation of the side group).

Acknowledgment. Financial support from the NSFC (nos. 20773022 and 20673120), the NCET-06-0321, the JLSDP (20082212), and the NENU-STB07007 is gratefully acknowledged.

Supporting Information Available: Tables S1−S4 listing results of the preliminary calculations, Figures S1−S3, and details on the calculation of the diameter of the tunnel. This material is available free of charge via the Internet at http://pubs.acs.org.

References and Notes

(1) Allcock, H. R. *Heteroatom Ring Systems and Polymers*; Academic Press: New York, 1967.

(2) Krishnamurthy, S. S.; Sau, A. C. *Adv. Inorg. Chem. Radiochem.* **1978**, *21*, 41.

(3) Allcock, H. R. *Phosphorus-Nitrogen Compounds. Cyclic, Linear, and High Polymeric Systems*; Academic Press: New York, 1972.
(4) Gleria, M. *Recent Adv. Macromol.* **2000**, *1*, 103.
(5) Allen, C. W. In *The Chemistry of Inorganic Homo- and Hetero-Cycles*; Haiduc, I., Sowerby, D. B., Eds.; Academic Press: London, 1987; Vol. 2, p 501.
(6) Kobayashi, T.; Isoda, S.; Kubono, K. In *Comprehensive Supramolecular Chemistry*; MacNicol, D. D., Toda, F., Bishop, R., Eds.; Pergamon Press: United Kingdom, 1996.
(7) Chandrasekhar, V. *Adv. Polym. Sci.* **1998**, *135*, 139.
(8) Levallois-Gruetzmacher, J. In *Phosphazenes: A Worldwide Insight*; Gleria, S., De Jaeger, M. R., Eds.; NOVA Science Publishers: Hauppauge, NY, 2004.
(9) Inoue, K. *Prog. Polym. Sci.* **2000**, *25*, 453.
(10) Majoral, J. P.; Caminade, A. M. In *Phosphazenes: A Worldwide Insight*; Gleria, M., De Jaeger, R., Eds.; NOVA Science Publishers: Hauppauge, NY, 2002.
(11) Sozzani, P.; Comotti, A.; Bracco, S.; Simonutti, R. *Angew. Chem., Int. Ed.* **2004**, *43*, 2792.
(12) Blau, W. J.; Fleming, A. J. *Science.* **2004**, *304*, 1457.
(13) (a) Whitesides, G. M.; Grzybowski, B. *Science* **2002**, *295*, 2418. (b) Hertzsch, T.; Hulliger, J.; Weber, E.; Sozzani, P. Organic Zeolites. *Encyclopedia of Supramolecular Chemistry*; Marcel Dekker: New York, 2004; p 996.
(14) Chae, H. K.; Siberio-Perez, D. Y.; Kim, J. Y.; Eddaoudi, G. M.; Matzger, A. J.; O'Keeffe, M.; Yaghi, O. M. *Nature* **2004**, *427*, 523.
(15) Ward, M. D. *Science.* **2003**, *300*, 1104.
(16) Kuznicki, S. M.; Bell, V. A.; Nair, S.; Hillhouse, H. W.; Jacubinas, R. M.; Braunbarth, C. M.; Toby, B. H.; Tsapatsis, M. *Nature* **2001**, *412*, 720.
(17) (a) Allcock, H. R.; Siegel, L. A. *J. Am. Chem. Soc.* **1964**, *86*, 5140. (b) Allcock, H. R.; Stein, M. T. *J. Am. Chem. Soc.* **1974**, *96*, 49.
(18) Allcock, H. R.; Levin, M. L.; Whittle, R. R. *Inorg. Chem.* **1986**, *25*, 41.
(19) Sozzani, P.; Bracco, S.; Comotti, A.; Ferretti, L.; Simonutti, R. *Angew. Chem., Int. Ed.* **2005**, *44*, 1816.
(20) (a) Comotti, A.; Gallazzi, M. C.; Simonutti, R.; Sozzani, P. *Chem. Mater.* **1998**, *10*, 3589. (b) Meersmann, T.; Logan, J. W.; Simonutti, R.; Caldarelli, S.; Comotti, A.; Sozzani, P.; Kaiser, L. G.; Pines, A. *J. Phys. Chem. A* **2000**, *104*, 11665. (c) Sozzani, P.; Comotti, A.; Simonutti, R.; Meersmann, T.; Logan, J. W.; Pines, A. *Angew. Chem., Int. Ed* **2000**, *39*, 2695. (d) Comotti, A.; Bracco, S.; Mauri, M.; Ferretti, L.; Simonutti, R.; Sozzani, P. *Chem. Commun.* **2007**, 350. (e) Sozzani, P.; Comotti, A.; Bracco, S.; Simonutti, R. *Angew. Chem., Int. Ed.* **2004**, *43*, 2792.
(21) Couderc, G.; Behrnd, N. R.; Kramer, K.; Hulliger, J. *Microporous Mesoporous Mater.* **2005**, *88*, 170.
(22) Hertzsch, T.; Budde, F.; Weber, E.; Hulliger, J. *Angew. Chem., Int. Ed.* **2002**, *41*, 2281.
(23) Hertzsch, T.; Kluge, S.; Weber, E.; Budde, F.; Hulliger, J. *Adv. Mater.* **2001**, *13*, 1864.
(24) (a) Sozzani, P.; Comotti, A.; Bracco, S.; Simonutti, R. *Angew. Chem., Int. Ed.* **2004**, *43*, 2792. (b) Brustolon, M.; Barbon, A.; Bortolus, M.; Maniero, A. L.; Sozzani, P.; Comotti, A.; Simonutti, R. *J. Am. Chem. Soc.* **2004**, *126*, 155121.
(25) (a) Sozzani, P.; Comotti, A.; Bracco, S.; Simonutti, R. *Chem. Commun.* **2004**, 768. (b) Comotti, A.; Simonutti, R.; Sozzani, P. *Chem. Mater.* **1999**, *11*, 1476.
(26) Allcock, H. R.; Stein, M. T.; Stanko, J. A. *J. Am. Chem. Soc.* **1971**, *93*, 3173.
(27) Allcock, H. R.; Kugel, R. L. *Inorg. Chem.* **1966**, *5*, 1016.
(28) (a) Siegel, L. A.; van den Hende, J. H. *J. Chem. Soc. A* **1967**, 817. (b) Allcock, H. R.; Allen, R. W.; Bissel, E. C.; Smeltz, L. A.; Teeter, M. *J. Am. Chem. Soc.* **1976**, *98*, 5120.
(29) Breza, M. *J. Mol. Struct. (Theochem)* **2000**, *505*, 169.
(30) Breza, M. *Polyhedron* **2000**, *19*, 389.
(31) Luana, L.; Pendas, A. M.; Costales, A. *J. Phys. Chem. A* **2001**, *105*, 5280.
(32) Waltman, R. J.; Lengsfield, B.; Pacansky, J. *Chem. Mater.* **1997**, *9*, 2185.
(33) Gervais, C.; Hertzsch, T.; Hulliger, J. *J. Phys. Chem. B* **2005**, *109*, 7961.
(34) (a) Allcock, H. R.; Primrose, A. P.; Silverberg, E.; Visscher, K. B. *Chem. Mater.* **2000**, *12*, 2530. (b) Kubono, K.; Asaka, N.; Isoda, S.; Kobayashi, T.; Taga, T. *Acta Crystallogr., Sect. C* **1994**, *324*, 50.
(35) Levchik, G. F.; Grigoriev, Y. V.; Balabanovich, A. I.; Levchik, S. V.; Klatt, M. *Polym. Int.* **2000**, *49*, 1095.
(36) Gahungu, G.; Zhang, B.; Zhang, J. *Chem. Phys. Lett.* **2004**, *388*, 422.
(37) Gahungu, G.; Zhang, B.; Zhang, J. *J. Phys. Chem. B* **2007**, *111*, 5031.
(38) Becke, A. D. *J. Chem. Phys.* **1993**, *98*, 1372.
(39) Rassolov, V. A.; Ratner, M. A.; Pople, J. A.; Redfern, P. C.; Curtiss, L. A. *J. Comput. Chem.* **2001**, *22*, 976.
(40) Hariharan, P. C.; Pople, J. A. *Mol. Phys.* **1974**, *27*, 209.
(41) Gordon, M. S. *Chem. Phys. Lett.* **1980**, *76*, 163.
(42) Foresman, J. B.; Head-Gordon, M.; Pople, J. A.; Frisch, M. J. *J. Phys. Chem.* **1992**, *96*, 135.
(43) McLean, A. D.; Chandler, G. S. *J. Chem. Phys.* **1980**, *72*, 5639.
(44) Krishnan, R.; Binkley, J. S.; Seeger, R.; Pople, J. A. *J. Chem. Phys.* **1980**, *72*, 650.
(45) Wachters, A. J. H. *J. Chem. Phys.* **1970**, *52*, 1033.
(46) Koopmans, T. *Physica* **1934**, *1*, 104.
(47) Frisch, M. J.; Trucks, G. W.; Schlegel, H. B.; Scuseria, G. E.; Robb, M. A.; Cheeseman, J. R. ; Montgomery J.A. Jr.; Vreven, T.; Kudin, K. N.; Burant, J. C.; Millam, J. M.; Iyengar, S. S.; Tomasi, J.; Barone, V.; Mennucci, B.; Cossi, M.; Scalmani, G.; Rega, N.; Petersson, G. A.; Nakatsuji, H.; Hada, M.; Ehara, M.; Toyota, K.; Fukuda, R.; Hasegawa, J.; Ishida, M.; Nakajima, T.; Honda, Y.; Kitao, O.; Nakai, H.; Klene, M.; Li, X.; Knox, J. E.; Hratchian, H. P.; Cross, J. B.; Bakken, V.; Adamo, C.; Jaramillo, J.; Gomperts, R.; Stratmann, R. E.; Yazyev, O.; Austin, A. J.; Cammi, R.; Pomelli, C.; Ochterski, J. W.; Ayala, P. Y.; Morokuma, K.; Voth, G. A.; Salvador, P.; Dannenberg, J. J.; Zakrzewski, V. G.; Dapprich, S.; Daniels, A. D.; Strain, M. C.; Farkas, O.; Malick, D. K.; Rabuck, A. D.; Raghavachari, K.; Foresman, J. B.; Ortiz, J. V.; Cui, Q.; Baboul, A. G.; Clifford, S.; Cioslowski, J.; Stefanov, B. B.; Liu, G.; Liashenko, A.; Piskorz, P.; Komaromi, I.; Martin, R. L.; Fox, D. J.; Keith, T.; Al.Laham, M. A.; Peng, C. Y.; Nanayakkara, A.; Challacombe, M.; Gill, P. M. W.; Johnson, B.; Chen, W.; Wong, M. W.; Gonzalez, C.; Pople, J. A. *Gaussian 03*, revision D.02; Gaussian, Inc.: Wallingford, CT, 2004.
(48) http://www.cscs.ch/molekel by Stephan Portmann, **2002**, CSCS/ETHZ.
(49) Tenderholt, A. L. *Pymolyze*, Version 2.0; Stanford University: Stanford, CA, 2007.
(50) *Materials Studio*; Accelrys Inc.: San Diego, CA, 2005.
(51) Sun, H.; Ren, P.; Friend, J. R. *Comput. Theor. Polym. Sci.* **1998**, *8*, 229.
(52) (a) Becke, A. D. *J. Chem. Phys.* **1993**, *98*, 5648. (b) Perdew, J. P. In *Electronic Structure of Solids*; Ziesche, P., Eschrig, H., Eds.; Akademie Verlag: Berlin, 1991.
(53) (a) Adamo, C.; Barone, V. *J. Chem. Phys.* **1999**, *110*, 61580. (b) Van Voorhis, T.; Scuseria, G. E. *J. Chem. Phys.* **1998**, *109*, 400.
(54) Trautner, F.; Singh, R. L.; Kirchmeier, R. P.; Shreeve, J. M.; Oberhammer, H. *Inorg. Chem.* **2000**, *39*, 5398.
(55) Belyakov, A. V.; Dalhus, B.; Haaland, A.; Shorokhov, D. J.; Volden, H. V. *J. Chem. Soc., Dalton Trans.* **2002**, 3756.
(56) (a) Allen, C. W.; Green, J. C. *Inorg. Chem.* **1980**, *19*, 1719. (b) Allen, C. W.; Brown, D. E.; Worley, S. D. *Inorg. Chem.* **2000**, *39*, 810.
(57) Fukui, K. *Theory of Orientation and Stereoselection, Reactivity and Structure, Concepts in Organic Chemistry*; Springer: Berlin, 1975; Vol. 2.
(58) Zhang, R. Q.; Lee, C. S.; Lee, S. T. *J. Chem. Phys.* **2000**, *112*, 8614.
(59) Lee, S. T.; Hou, X. Y.; Mason, M. G.; Tang, C. W. *Appl. Phys. Lett.* **1998**, *72*, 1593.
(60) Kubono, K.; Asaka, N.; Isoda, S.; Kobayashi, T. *Acta Crystallogr.* **1993**, *C49*, 404.

JP804185R